Electrical characterization of atomic layer deposited Al2O3/InN interfaces

Ye Jia, Amir M. Dabiran, and Uttam Singisetti

Citation: Journal of Vacuum Science & Technology A **34**, 01A133 (2016); doi: 10.1116/1.4936928
View online: http://dx.doi.org/10.1116/1.4936928
View Table of Contents: http://scitation.aip.org/content/avs/journal/jvsta/34/1?ver=pdfcov
Published by the AVS: Science & Technology of Materials, Interfaces, and Processing

Articles you may be interested in

Rectification and tunneling effects enabled by Al2O3 atomic layer deposited on back contact of CdTe solar cells
Appl. Phys. Lett. **107**, 013907 (2015); 10.1063/1.4926601

Passivation of In0.53Ga0.47As/ZrO2 interfaces by AlN atomic layer deposition process
J. Appl. Phys. **114**, 034107 (2013); 10.1063/1.4815934

Atomic layer deposition of Al2O3 on GaSb using in situ hydrogen plasma exposure
Appl. Phys. Lett. **101**, 231601 (2012); 10.1063/1.4768693

Effective passivation of In0.2Ga0.8As by HfO2 surpassing Al2O3 via in-situ atomic layer deposition
Appl. Phys. Lett. **101**, 172104 (2012); 10.1063/1.4762833

Studies on atomic layer deposition Al2O3/In0.53Ga0.47As interface formation mechanism based on air-gap capacitance-voltage method
Appl. Phys. Lett. **101**, 122102 (2012); 10.1063/1.4753927

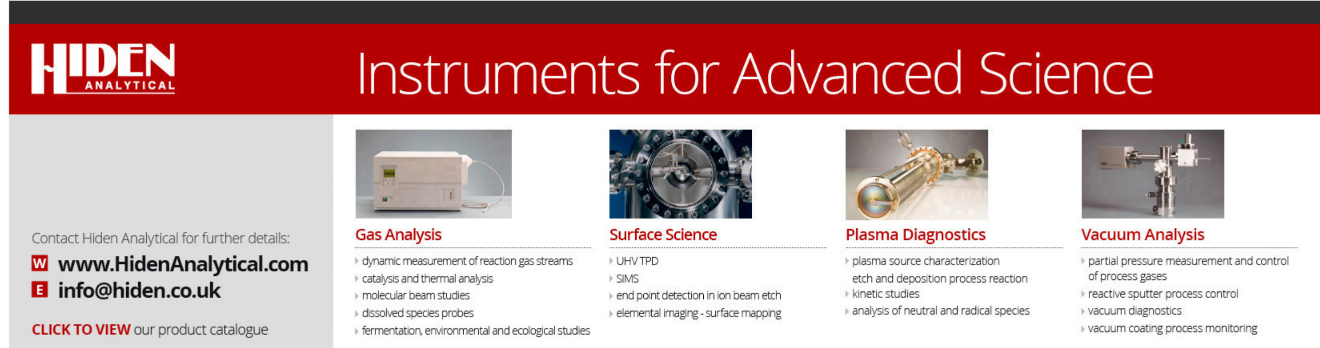

Redistribution subject to AVS license or copyright; see http://scitation.aip.org/termsconditions. Download to IP: 128.205.187.181 On: Wed, 02 Dec 2015 14:47:49

Electrical characterization of atomic layer deposited Al_2O_3/InN interfaces

Ye Jia
Electrical Engineering Department, University at Buffalo, Buffalo, New York 14260

Amir M. Dabiran
SVT Associates Inc., Eden Prairie, Minnesota 55344

Uttam Singisetti[a]
Electrical Engineering Department, University at Buffalo, Buffalo, New York 14260

(Received 31 August 2015; accepted 19 November 2015; published 2 December 2015)

In this article, the authors report the electrical properties of atomic layer deposited Al_2O_3/InN interfaces evaluated by capacitance–voltage (C-V), current–voltage (I-V), and x-ray photoemission spectroscopy techniques. I-V characteristics show low leakage currents ($300\,pA/\mu m^2$) in the deposited dielectrics. However, C-V curves show that *ex situ* surface treatments with hydrochloric acid, ammonium sulfide, and hydrobromic acid has little effect on the surface electron accumulation layer, with an estimated interface state density over $4 \times 10^{13}/cm^2$. The effect of the surface treatments on valance band offset between Al_2O_3 and InN was also investigated. © *2015 American Vacuum Society*.
[http://dx.doi.org/10.1116/1.4936928]

I. INTRODUCTION

The low electron effective mass[1] and predicted high electron velocities[2–4] in InN make it attractive for future terahertz electronic devices. However, very few experimental electronic devices have been demonstrated because of a number of challenges, which include high unintentional doping,[4,5] difficulty of p-type doping,[6,7] and large surface pinning.[5,7–9] Extreme band bending of InN due to the high surface charge densities impede field effect modulation of the bulk electrons.[5,7,8] The presence of surface electron accumulation layer also makes it difficult to use conventional methods for determining the bulk carrier properties in p-type InN.[6,10] By optimizing the growth condition and by p-type doping, surface electron concentration at surface has been reduced;[6,11,12] however, the concentration is still high for device applications.

The large surface accumulation layer has been attributed to the surface defects (In–O and In–In bonds) on the surface.[9,13–16] Removal of the surface defects by chemical treatments could reduce the pinning in InN. Numerous papers have shown by spectroscopy analysis that acids and bases can effectively remove the native oxide on III–V and III–N semiconductor surface by reacting with the surface atoms.[15–19] After careful chemical treatments, partially unpinning of the InN has also been reported by spectroscopic analysis.[15–18] The surface defects can also be removed by *in situ* trimethylaluminum (TMA) prepulsing in an atomic layer deposition (ALD) tool. TMA prepulsing has been successfully used to passivate III–V semiconductors.[20,21] Recently, the reduction of band bending in InN nanowire has been reported.[22] P-channel device has also been realized in nanowire and exhibits good field effect modulation of the electrons.[23,24] However, the FET devices on InN epitaxial film have not been demonstrated.

In this article, we report on the electrical properties of atomic layer deposited Al_2O_3 on InN surface. ALD deposited high-k oxides are widely used as gate dielectrics in silicon metal oxide semiconductor field effect transistors,[25–28] and have been used to obtain low interface state density interfaces to III–Vs and GaN.[21,29–32] Previous report on ALD dielectrics on InN primarily focused on the structural properties.[33] Here, we focus on the capacitance–voltage (C-V) and current–voltage (I-V) characteristics that are essential to understand in order to achieve practical electronic devices. The effect of surface treatments on C-V, I-V, and band-offset was investigated.

II. EXPERIMENTAL DETAILS

The cross-section schematic of the In-polar InN metal-oxide-semiconductor capacitor (MOSCAP) structure used in this study is shown in Fig. 1(a). A 500 nm of InN layer was grown by plasma assisted molecular beam epitaxy on sapphire substrate with an AlN nucleation layer and 500 nm of GaN buffer. The GaN buffer was grown at 730 °C at a growth rate of 0.7 m/h, while the InN layer was grown at 340 °C with In:N ratio of 1:1 at the growth rate of 0.38 m/h. X-ray diffraction measurements confirm the wurtzite growth. The polarity of the sample was verified by potassium hydroxide (KOH) etching.[34] Figures 1(b) and 1(c) show the secondary electron microscopy (SEM) and atomic force microscopy (AFM) images of the In-polar InN surface indicating a rough surface.

MOSCAP structures [shown in Fig. 1(a)] were used to study the dielectric–InN interface. A 30 nm layer of Al_2O_3 was deposited by thermal ALD at 300 °C in a Cambridge Savannah S100 system using TMA and water (H_2O) precursors. Prior to the deposition of Al_2O_3, the samples were treated by different acids and bases to remove surface defects. Reference 16 reports that hydrochloric acid (HCl) can remove the indium metal adlayer on top of InN and reduce surface pinning significantly in N-polar InN.

a)Electronic mail: uttamsin@buffalo.edu

Redistribution subject to AVS license or copyright; see http://scitation.aip.org/termsconditions. Download to IP: 128.205.187.181 On: Wed, 02 Dec 2015 14:47:49

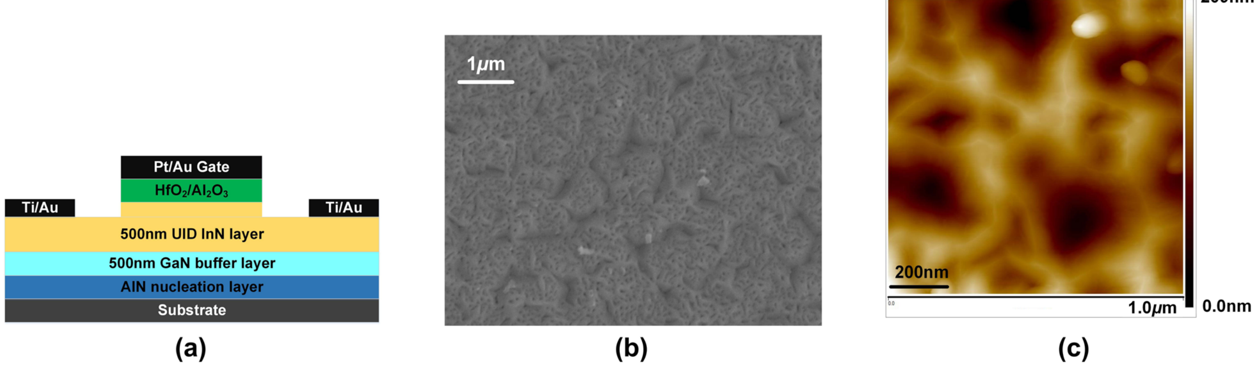

FIG. 1. (Color online) (a) Cross-section schematic of InN MOSCAP device. (b) SEM and (c) AFM image of the InN surface.

Reduced surface bending has also been reported in InN after ammonia sulfide [$(NH_4)_2S$] treatment because of the formation of In-S dipole near the surface.[15,17] Hydrobromic acid (HBr) has been used to remove the native oxide on GaAs surface.[19] As discussed previously, *in situ* TMA prepulsing has also been used to passivate III–V semiconductors. Therefore, we explore the effects of TMA, HCl, $(NH_4)_2S$, and HBr on the electrical properties of InN MOSCAPs.

All samples were first cleaned by buffered HF for 4 min to remove surface contaminants and oxides. Sample B, C and D were dipped in HCl (∼15% w/w) at 50 °C for 10 min. Sample E was subjected to HBr (∼48% w/w) at 50 °C for 10 min instead of HCl. Samples D and E were then treated by $(NH_4)_2S$ (∼44% w/w) at 50 °C for 1 h. Twenty cycles of TMA were pulsed on samples C, D, and E before starting the normal Al_2O_3 deposition. A summary of the various surface treatments studied here is given in Table I. All the samples were capped with 5 nm HfO_2 layer to protect the Al_2O_3 during subsequent photolithography process. Next, Pt/Au top electrodes were deposited by lift-off technique for the top anode contact. The bottom Ti/Au contacts were deposited after etching the oxide and InN layers by BCl_3/Ar based reactive ion etching process.

We calculated the band-offsets of the deposited Al_2O_3 on InN by x-ray photoelectron spectroscopy (XPS). The XPS spectra were acquired by using a Physical Electronic PHI VersaProbe 5000 equipped with a hemispherical energy analyzer. A monochromatic Al Kα (1486.6 eV) operated at 25.3 W and 15 kV was used. The high resolution spectra were obtained by operating the energy analyzer at a pass energy of 11.75 eV. The energy resolution was 0.025 eV. The acquisition was done under ultrahigh vacuum environment (operating pressure was lower than 4.0×10^6 Pa). Dual charge neutralization was used to correct the surface charging effects. The binding energies were also aligned by setting the CH_x peak in C 1*s* envelope at 285 eV.[35] However, the band offset measurements were not affected by the charging effects.

TABLE I. Summary of the chemical treatments.

Sample	Treatment
A	HF
B	HF, HCl
C	HF, HCl, TMA
D	HF, HCl, $(NH_4)_2S$, TMA
E	HF, HBr, $(NH_4)_2S$, TMA

The valence band offset (VBO) was extracted by the method proposed by Kraut *et al.*[36]

$$\Delta E_v = (E^{Al\,2p}_{Al_2O_3/InN} - E^{In\,3d_{5/2}}_{Al_2O_3/InN}) + (E^{In\,3d_{5/2}}_{InN} - E^{VBM}_{InN}) - (E^{Al\,2p}_{Al_2O_3} - E^{VBM}_{Al_2O_3}), \quad (1)$$

where the superscripts indicate the XPS peaks and the subscripts indicate the corresponding samples. Here, we used Al 2*p* and In $3d_{5/2}$ as the core levels in InN and Al_2O_3. Three different samples were required: 45 nm Al_2O_3 on Si, bare InN, and ∼2 nm Al_2O_3 on InN to calculate the term of $(E^{Al\,2p}_{Al_2O_3} - E^{VBM}_{Al_2O_3})$, $(E^{In\,3d_{5/2}}_{InN} - E^{VBM}_{InN})$, and $(E^{Al\,2p}_{Al_2O_3/InN} - E^{In\,3d_{5/2}}_{Al_2O_3/InN})$, respectively. The conduction band offset (CBO) was giving by

$$\Delta E_c = \Delta E_g - \Delta E_v, \quad (2)$$

where the ΔE_g is the difference in band gap and ΔE_v is the valence band discontinuity. The core level and loss structure of O 1*s* on the 45 nm Al_2O_3/Si sample were acquired in order to find the band gap of Al_2O_3. From the onset energy of the loss energy spectrum, the band gap of insulator can be found.[35]

The electrical properties of the interfaces were characterized at room temperature. The current–voltage measurements were done by using Agilent 4155B-41501B semiconductor parameter analyzer. The leaking current was examined in a large voltage range. The capacitance–voltage measurements were carried out using Agilent 4294A Precision Impedance Analyzer, the measurement frequencies were set from 10 kHz to 5 MHz, and the signal level was set to 20 mV root mean square.

III. RESULTS AND DISCUSSION

Figures 2(a)–2(c) show XPS peaks from 45 nm Al_2O_3 on Si, bare InN, and ∼2 nm Al_2O_3/InN heterostructure after HF

Redistribution subject to AVS license or copyright; see http://scitation.aip.org/termsconditions. Download to IP: 128.205.187.181 On: Wed, 02 Dec 2015 14:47:49

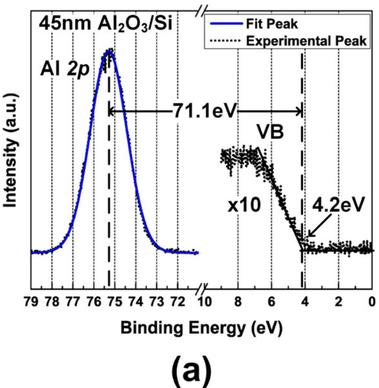

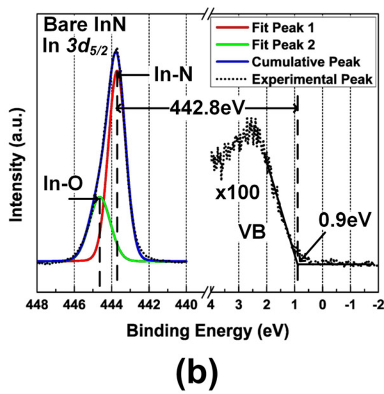

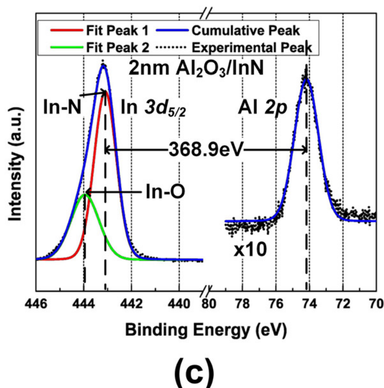

FIG. 2. (Color online) XPS peaks used to calculate valance band offset. (a) In $3d_{5/2}$ peak and valance band minimum obtained from InN. (b) Al $2p$ and valance band minimum in 45 nm Al_2O_3 on Si. (c) Al $2p$ and (d) In $3d_{5/2}$ in 2 nm Al_2O_3/InN heterostructure after HF treatment. The VBO was found to be 2.8 eV. In $3d_{5/2}$ peaks in (b) and (c) showed In-O peak.

cleaning, respectively. The XPS spectra were curved fitted with a Voigt band type after Shirley background subtraction with the following limits: binding energy ±0.4 eV, FWHM ±0.2 eV, and 92% Gauss. The valence band maxima (VBM) was found by linearly extrapolating the leading edge of the XPS spectra.[37] In Fig. 2(b), the In $3d_{5/2}$ spectrum showed a strong peak at 443.7 eV correspond to In–N bond[6,38–41] and a second peak at 444.7 eV corresponding to In–O bond,[17] indicating the presence of InO_x layer on top of InN. The VBM was found to be 0.9 eV below Fermi level, suggesting downward band bending near surface due to the high density of surface states. From XPS spectra, the $(E^{Al2p}_{Al_2O_3} - E^{VBM}_{Al_2O_3})$, $(E^{In3d_{5/2}}_{InN} - E^{VBM}_{InN})$, and $(E^{Al2p}_{Al_2O_3/InN} - E^{In3d_{5/2}}_{Al_2O_3/InN})$ were calculated to be 71.1, 442.8, and −368.9 eV, giving a VBO (ΔE_v) of 2.8 eV. Figure 3 shows the core level and loss structure of O 1s on the 45 nm Al_2O_3/Si sample. The band gap of Al_2O_3 was determined to be ~7 eV, which was in good agreement with the literature reported values.[35] Taking the band gap of InN to be 0.7 eV, the CBO (ΔE_c) was calculated to be

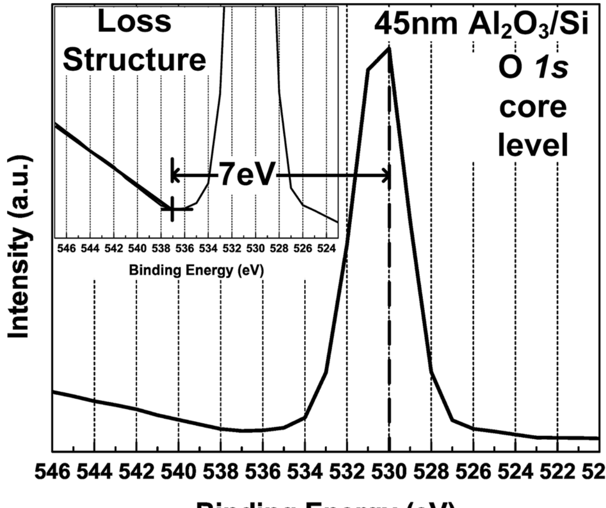

FIG. 3. O 1s peaks acquired from the 45 nm Al_2O_3/Si sample to determine the bandgap of Al_2O_3. The inset shows the loss structure. The bandgap of Al_2O_3 was determined to be 7 eV.

3.5 eV. Table II gives the calculated VBO and CBO between Al_2O_3 and InN for the different samples. All the samples show a similar VBO of 2.16 ~ 2.24 eV except the HF treated sample. A higher VBO was seen in HF treated sample, which could be due to the insufficient removal of native indium oxides. In fact, all the In $3d_{5/2}$ peaks showed the presence of In–O bond. It is possible that the oxygen was adsorbed onto the surface during the transfer to ALD chamber after the removal of the native oxide by the acids and bases. Figure 4 shows the XPS spectra of the samples B and C. The ratio of the integrated area of In–N and In–O was calculated to be ~1.5 for sample B and ~1.8 for sample C. The TMA pretreatment did show a reduction in the intensity of In–O peak, but the presence of In–O suggested insufficient pretreatment.

Figure 5 shows the measured I-V of the devices. From −20 V to +8 V, the leakage current was below 0.01 pA/μm^2. Surface morphology has been reported to lead to leaky dielectrics in N-polar GaN films.[42] No such degradation in the dielectric insulating properties was observed for InN. After +8 V, the current increased rapidly and behaved like diode. Although there was dispersion among different treatments, the leakage was below 300 pA/μm^2.

The room temperature C-V curve of the InN MOSCAP with TMA pretreatment (sample C) measured at 1 MHz is shown in Fig. 6(a). No indication of depletion of surface electron layer or bulk electron density was observed in the C-V curve. Figure 6(b) shows the relative change in the capacitance [$\Delta C/C = (C - C_{min})/C_{min}$] for all the MOSCAPs studied here. All samples showed similar behavior: capacitance first decreased slightly until −1.5 V and further

TABLE II. Calculation of the VBO and CBO with surface treatments.

Sample	VBO (eV)	CBO (eV)
A	2.8	3.5
B	2.16	4.14
C	2.21	4.09
D	2.23	4.07
E	2.24	4.06

Redistribution subject to AVS license or copyright; see http://scitation.aip.org/termsconditions. Download to IP: 128.205.187.181 On: Wed, 02 Dec 2015 14:47:49

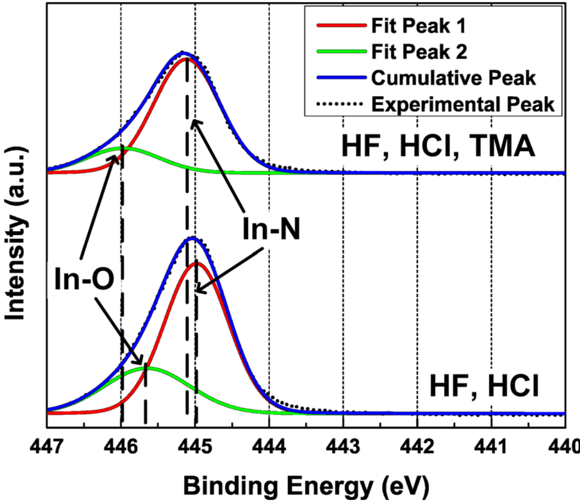

FIG. 4. (Color online) XPS spectra of the 2 nm Al_2O_3/InN heterostructure after HF, HCl, and TMA treatments and after HF and HCl treatments. The TMA treated sample showed reduced In–O bond.

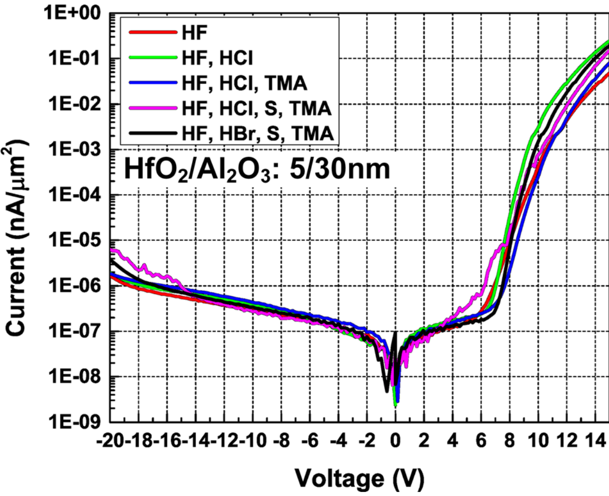

FIG. 5. (Color online) I-V curves of the devices on the InN. I-V curves showed very small current leakage, indicating good insulating property of the dielectric layer.

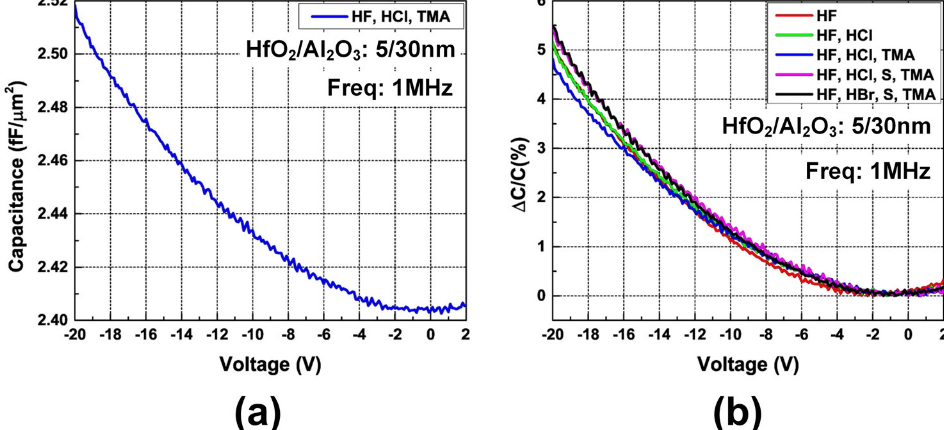

FIG. 6. (Color online) (a) C-V profile of the device on the TMA pretreated sample. Depletion of electrons does not occur even at large gate bias. (b) Variation of the capacitance with respect to the minimal capacitance. The C-V curves with different treatments show similar trend. Regardless of surface treatments, the percentage of capacitance variation ended at ~5% when bias is −20 V with no indication of depletion of InN.

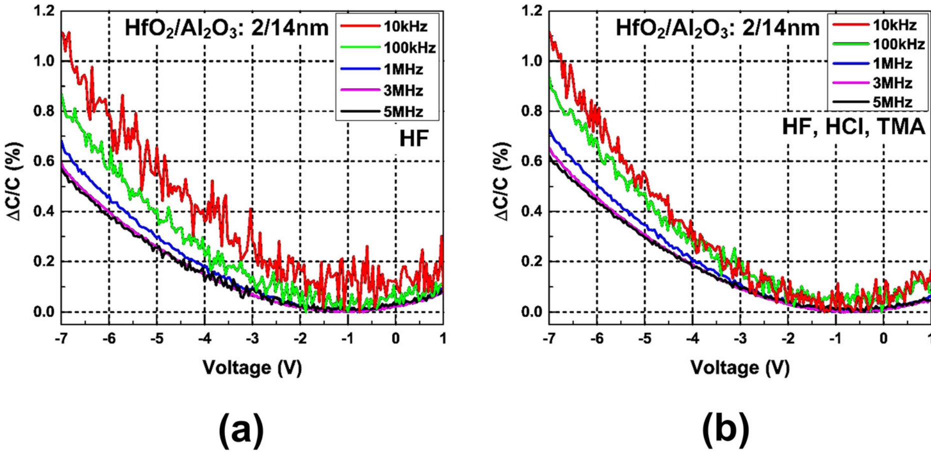

FIG. 7. (Color online) Frequency dependent C-V curves measured from (a) sample A and (b) sample C. The C-V curves did not show the depletion of surface electrons.

Redistribution subject to AVS license or copyright; see http://scitation.aip.org/termsconditions. Download to IP: 128.205.187.181 On: Wed, 02 Dec 2015 14:47:49

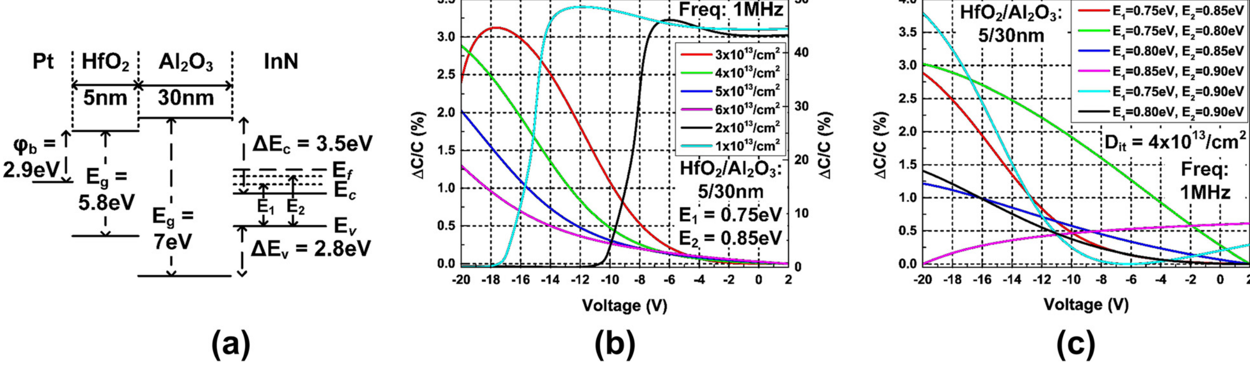

FIG. 8. (Color online) (a) Band diagram of the InN-MOSCAP with interface traps. (b) Simulated C-V curves with different interface state densities. The interface traps were inserted at 0.75 and 0.85 eV above valence band maximum. The densities varied from $1 \times 10^{13}/cm^2$ to $6 \times 10^{13}/cm^2$. (c) Simulated C-V curves with different locations of interface traps with a total density of $4 \times 10^{13}\ cm^{-2}$. Both the density and location affect the C-V profiles.

decreasing of the bias voltage results in increasing of capacitance. Irreversible dielectric breakdown was observed (not shown) at a reverse bias of 23 V. The surface treatments did not seem to significantly modify the pinning to observe bulk electron depletion although some shifts in the peak positions were observed in XPS. The increase in capacitance at higher reverse biases was attributed to the contribution of the interface states to the capacitance (C_{it}). The frequency dependent C-V curves of samples A and C are shown in Figs. 7(a) and 7(b), respectively. There is slight drop in $\Delta C/C$ from 10 kHz to 5 MHz; however, the variations were too small to reflect any depletion of the surface electrons. Other samples have similar frequency dispersion curves (not shown). All of the C-V curves did not show any depletion of the surface accumulation layer after surface treatments.

Simulations of C-V profiles were performed at 1 MHz in InN-MOSCAPs using Silvaco Atlas.[43] The oxide layer consisted of 30 nm Al_2O_3 and 5 nm HfO_2. Figure 8(a) shows the schematic of the band diagram of the InN MOSCAP with interface traps. The dielectric constants of Al_2O_3, HfO_2, and InN were 9, 12, and 8.4.[44] The electron affinities of Al_2O_3, HfO_2, and InN were 2.6,[45] 2.8,[46] and 5.8 eV.[47] The work function of Pt was taken to be 5.65 eV.[43] Two levels of the interface traps were inserted at 0.75 and 0.85 eV above valence band maximum. Figure 8(b) shows the simulated C-V curves for interface state densities (D_{it}) from $1 \times 10^{13}/cm^2$ to $6 \times 10^{13}/cm^2$. It can be seen that for $D_{it} > 4 \times 10^{13}/cm^2$, no depletion was observed in the C-V curves; however, at an interface density of $3 \times 10^{13}/cm^2$, the depletion of bulk electrons could be observed. By comparing Fig. 6(b) and Fig. 8(b), the D_{it} in our InN sample was high ($>4 \times 10^{13}/cm^2$). However, at a voltage of -20 V, the measured values of $\Delta C/C$ in Fig. 6(b) were higher than the values in Fig. 8(b). Therefore, we simulated the C-V curves with interface traps at different positions with a total density of $4 \times 10^{13}\ cm^{-2}$, which is shown in Fig. 8(c). As seen, the increment in capacitance depends on the exact location of interface traps. Since our measured data exhibited large $\Delta C/C$ values, we can conclude that the interface traps inside our InN sample were distributed in a large energy range above conduction band minimum with a very high density. The high density of interface trap leads to the failure of capacitance or conductance method in evaluating the density of the interface traps.

From the measured C-V profiles, the surface treatments did not show significant change in the pinning of InN. Unlike the reported unpinning by surface treatments analyzed using XPS technique,[15–18] the InN samples studied here were not transferred to ALD chamber under vacuum. This could lead to oxidation of the InN surface and pinning of the interface. Further oxidation of the surface can also occur during the heating of the samples in ALD chamber where the background pressure was in milliTorr range. Surface treatment followed by vacuum annealing and transfer under vacuum to ALD could lead to unpinning in MOSCAPs.

IV. CONCLUSIONS

We studied the capacitance–voltage and current–voltage characteristics of In-polar InN/Al_2O_3 MOSCAPs with different *ex situ* surface treatments. Hydrochloric acid, ammonium sulfide, hydrobromic acid, and trimethylaluminum treatments were explored. Although the I-V measurements of the MOSCAPs show low leakage currents, C-V profile indicates no significant change in the pinning of InN surface due to these surface treatments.

ACKNOWLEDGMENTS

This work was supported by U.S. Office of Naval Research (ONR) Grant (N000141310214) monitored by Paul Maki. The authors would like to thank Joseph A. Gardella, Jr., at the University at Buffalo (UB) for providing access to the XPS instrumentation for analyzing the samples reported here. The XPS was funded by an NSF MRI Grant No. CHE 1048740.

[1] S. P. Fu and Y. F. Chen, Appl. Phys. Lett. **85**, 1523 (2004).
[2] S. K. O'Leary, B. E. Foutz, M. S. Shur, and L. F. Eastman, J. Mater. Sci.: Mater. EL **17**, 87 (2006).
[3] N. Khan, A. Sedhain, J. Li, J. Y. Lin, and H. X. Jiang, Appl. Phys. Lett. **92**, 172101 (2008).
[4] V. Lebedev, V. Cimalla, T. Baumann, O. Ambacher, F. M. Morales, J. G. Lozano, and D. González, J. Appl. Phys. **100**, 094903 (2006).
[5] P. D. C. King, T. D. Veal, and C. F. McConville, J. Phys. Condens. Mater. **21**, 174201 (2009).

Redistribution subject to AVS license or copyright; see http://scitation.aip.org/termsconditions. Download to IP: 128.205.187.181 On: Wed, 02 Dec 2015 14:47:49

[6]S. Choi, F. Wu, O. Bierwagen, and J. S. Speck, J. Vac. Sci. Technol. A **31**, 031504 (2013).
[7]T. D. Veal, L. F. J. Piper, W. J. Schaff, and C. F. McConville, J. Cryst. Growth **288**, 268 (2006).
[8]I. Mahboob, T. D. Veal, L. F. J. Piper, C. F. McConville, H. Lu, W. J. Schaff, J. Furthmüller, and F. Bechstedt, Phys. Rev. B **69**, 201307(R) (2004).
[9]C. G. Van de Walle and D. Segev, J. Appl. Phys. **101**, 081704 (2007).
[10]C. A. Hurni, S. Choi, O. Bierwagen, and J. S. Speck, Appl. Phys. Lett. **100**, 082106 (2012).
[11]G. Koblmüller, C. S. Gallinat, S. Bernardis, J. S. Speck, G. D. Chern, E. D. Readinger, H. Shen, and M. Wraback, Appl. Phys. Lett. **89**, 071902 (2006).
[12]A. Yang, Y. Yamashita, T. Yamaguchi, M. Imrua, M. Kaneko, O. Sakata, Y. Nanishi, and K. Kobayashi, Appl. Phys. Express **5**, 031002 (2012).
[13]V. Lebedev *et al.*, Phys. Status Solidi C **5**, 495 (2008).
[14]C.-L. Wu, H.-M. Lee, C.-T. Kuo, C.-H. Chen, and S. Gwo, Phys. Rev. Lett. **101**, 106803 (2008).
[15]L. R. Bailey, T. D. Veal, C. E. Kendrick, S. M. Durbin, and C. F. McConville, Appl. Phys. Lett. **95**, 192111 (2009).
[16]C.-T. Kuo, S.-C. Lin, K.-K. Chang, H.-W. Shiu, L.-Y. Chang, C.-H. Chen, S.-J. Tang, and S. Gwo, Appl. Phys. Lett. **98**, 052101 (2011).
[17]Y.-H. Chang, Y.-S. Lu, Y.-L. Hong, C.-T. Kuo, S. Gwo, and J. A. Yeh, J. Appl. Phys. **107**, 043710 (2010).
[18]A. Eisenhardt, M. Himmerlich, and S. Krischok, Phys. Status Solidi A **209**, 45 (2012).
[19]A. Delabie *et al.*, J. Electrochem. Soc. **155**, H937 (2008).
[20]J. B. Clemens, E. A. Chagarov, M. Holland, R. Droopad, J. Shen, and A. C. Kummel, J. Chem. Phys. **133**, 154704 (2010).
[21]Y. Hwang, R. Engel-Herbert, and S. Stemmer, Appl. Phys. Lett. **98**, 052911 (2011).
[22]S. Zhao, S. Fathololoumi, K. H. Bevan, D. P. Liu, M. G. Kibria, Q. Li, G. T. Wang, H. Guo, and Z. Mi, Nano Lett **12**, 2877 (2012).
[23]B. H. Le, S. Zhao, N. H. Tran, T. Szkopek, and Z. Mi, Appl. Phys. Express **8**, 061001 (2015).
[24]S. Zhao, B. H. Le, D. P. Liu, X. D. Liu, M. G. Kibria, T. Szkopek, H. Guo, and Z. Mi, Nano Lett**13**, 5509 (2013).
[25]Y. Kim *et al.*, *IEDM '01. Technical Digest* (2001), p. 455.
[26]E. P. Gusev, E. Cartier, D. A. Buchanan, M. Gribelyuk, M. Copel, H. Okorn-Schmidt, and C. D'Emic, Microelectron. Eng. **59**, 341 (2001).
[27]E. P. Gusev, C. Cabral, Jr., M. Copel, C. D'Emic, and M. Gribelyuk, Microelectron. Eng. **69**, 145 (2003).
[28]J. Kavalieros *et al.*, *Symposium of the VLSI Technology: Digest of Technical Papers* (2006), p. 50.
[29]P. D. Ye, B. Yang, K. K. Ng, J. Bude, G. D. Wilk, S. Halder, and J. C. M. Hwang, Appl. Phys. Lett. **86**, 063501 (2005).
[30]H. D. Trinh *et al.*, Appl. Phys. Lett. **97**, 042903 (2010).
[31]M. Milojevic, C. L. Hinkle, F. S. Aguirre-Tostado, H. C. Kim, E. M. Vogel, J. Kim, and R. M. Wallace, Appl. Phys. Lett. **93**, 252905 (2008).
[32]H. D. Lee, T. Feng, L. Yu, D. Mastrogiovanni, A. Wan, T. Gustafsson, and E. Garfunkel, Appl. Phys. Lett. **94**, 222108 (2009).
[33]K. Okubo, A. Kobayashi, J. Ohta, H. Fujika, and M. Oshima, Appl. Phys. Express **4**, 091002 (2011).
[34]D. Muto, T. Araki, H. Naoi, F. Matsuda, and Y. Nanishi, Phys. Status Solidi A **202**, 773 (2005).
[35]T. Kamimura, K. Sasaki, M. H. Wong, D. Krishnamurthy, A. Kuramata, T. Masui, S. Yamakoshi, and M. Higashiwaki, Appl. Phys. Lett. **104**, 192104 (2014).
[36]E. A. Kraut, R. W. Grant, J. R. Waldrop, and S. P. Kowalczyk, Phys. Rev. Lett. **44**, 1620 (1980).
[37]S. A. Chambers, T. Droubay, T. C. Kaspar, and M. Gutowski, J. Vac. Sci. Technol. B **22**, 2205 (2004).
[38]A. Eisenhardt, G. Eichapfel, M. Himmerlich, A. Knübel, T. Passow, C. Wang, F. Benkhelifa, R. Aidam, and S. Krischok, Phys. Status Solidi C **9**, 685 (2012).
[39]P. D. C. King, T. D. Veal, P. H. Jefferson, C. F. McConville, T. Wang, P. J. Parbrook, H. Lu, and W. J. Schaff, Appl. Phys. Lett. **90**, 132105 (2007).
[40]T. Nagata, G. Koblmüller, O. Bierwagen, C. S. Gallinat, and J. S. Speck, Appl. Phys. Lett. **95**, 132104 (2009).
[41]A. L. Yang *et al.*, Appl. Phys. Lett. **94**, 163301 (2009).
[42]C. R. English, V. D. Wheeler, N. Y. Garces, N. Nepal, A. Nath, J. K. Hite, M. A. Mastro, and C. R. Eddy, Jr., J. Vac. Sci. Technol. B **32**, 03D106 (2014).
[43]Silvaco Inc., ATLAS user's manual, DEVICE SIMULATION software, 2011.
[44]V. W. L. Chin, T. L. Tansley, and T. Osotchan, J. Appl. Phys. **75**, 7365 (1994).
[45]M. L. Huang, Y. C. Chang, C. H. Chang, T. D. Lin, J. Kwo, T. B. Wu, and M. Hong, Appl. Phys. Lett. **89**, 012903 (2006).
[46]Y. C. Chang *et al.*, Appl. Phys. Lett. **92**, 072901 (2008).
[47]A. Belabbes, J. Furthmüller, and F. Bechstedt, Phys. Rev. B **84**, 205304 (2011).

Redistribution subject to AVS license or copyright; see http://scitation.aip.org/termsconditions. Download to IP: 128.205.187.181 On: Wed, 02 Dec 2015 14:47:49